

EXPERIMENTAL VALIDATION OF A HEAT AND MOISTURE MODEL FOR SOIL

Olukayode D. Akinyemi*

Thermal Systems Laboratory
Department of Mechanical Engineering,
Pontifical Catholic University of Parana
Rua Imaculada Conceição, 1155, Curitiba, PR 80215-901, Brazil
olukayodewumi@yahoo.com

Nathan Mendes

Thermal Systems Laboratory - LST
Pontifical Catholic University of Parana – PUCPR/CCET
Rua Imaculada Conceição, 1155
Curitiba – PR – 80215-901 – Brazil
nathan.mendes@pucpr.br

Abstract. Knowledge about the dynamics of soil moisture and heat especially at the surface provides important insight into the physical processes governing their interactions with the atmosphere, thereby improving the understanding of patterns of climate dynamics. In this context the paper presents the numerical and field experimental results of temperature and moisture evolution, which were measured on the surface of a sandy soil at Abeokuta, south-western Nigeria. An unconditionally stable numerical method was used, which linearizes the vapour concentration driving-potential term giving the moisture exchanged at the boundaries in terms of temperature and moisture content, and simultaneously solves the governing equations for each time step. Instantaneous temperature measurements were made at the surface using a thermocouple while the gravimetric method was employed to determine the volumetric water contents at some specific hours of the experimental period. The observed experimental data compared fairly well with the predicted values, with both having correlation coefficients greater than 0.9 and consequently following a common diurnal trend. The sensitivity of the model was very high to the choice of simulation parameters especially grid size refinement and time step. While the model underestimated the soil moisture content at 6 a.m. and 10 p.m., the measured temperatures were however overestimated. When compared to moisture content, average errors for temperature were low resulting in a minimal absolute difference in amplitude of 0.81°C.

Keywords. Heat and moisture transfer, unsaturated soils, experimental and numerical analysis.

1. Introduction

Following the phenomenological model of combined heat and moisture transfer in porous media as developed by Philip and de Vries (1957) and de Vries (1958, 1987), successful attempts have also been made by other authors to extend advanced research on the subject (Cassel *et al.*, 1969; Jackson *et al.*, 1974; Whitaker, 1977; Jury and Letey, 1979; Przesmycki *et al.*, 1985; Nassar and Horton, 1989; Nassar *et al.*, 1992a, 1992b; Yamanaka *et al.*, 1999). Heat transfer and moisture movement in unsaturated soils are closely related, with the particular hydrological and physical characteristics of the soil, and the atmospheric variables subject to the prevailing climatic conditions playing major roles. The model developed by Wu and Nofziger (1999) used the average water content of each layer as the major requirement to predict soil daily mean temperatures at different depths in the Hebei province of China, with the model giving a fairly good prediction of the measured temperatures. The surface layer of soil is of paramount importance and a vital ingredient in this environment is the detailed knowledge of the moisture and temperature regime, and the factors controlling them.

When moisture is present in the soil, it implies an additional mechanism: in the pores of unsaturated soil, liquid water evaporates at the warm side, absorbing latent heat of vaporization, while because of the vapour-pressure gradient, vapour condenses on the coldest side of the pore, releasing latent heat of vaporization (Deru and Kirkpatrick, 2002).

Heat and mass conservation equations have always been solved iteratively by using the values of temperature and moisture content from previous iterations to calculate the source terms, but usually not without the attendant complications connected with stability problems when long-term simulations are carried out with high time steps, especially at highly permeable surfaces (Rubin, 1968; Yoon *et al.*, 2003; Lu *et al.*, 2005; Griffol *et al.*, 2005). Kerestecioglu and Gu (1989) also investigated this phenomenon using evaporation-condensation theory but the application of this theory is only limited to low moisture content. Hence, Santos and Mendes (2005) obtained a linearized set of equations, by finite volume method and used the MultiTriDiagonal-Matrix Algorithm (MTDMA), which is an unconditionally stable numerical method, developed by Mendes and Philippi (2003) to describe the physical phenomena of heat and mass transfer in porous soils. Although, this model theoretically presents fast converging results, its validation has not been tested with experimental observations. The study therefore compares the numerically computed results with experimentally measured values of soil temperature and moisture content distributions determined at the surface of a tropical soil, with an ultimate aim of building a reference data-

base system for these physical quantities which are presently scarce in Nigeria due to cost and labour intensiveness of their long-term measurements.

2. Mathematical model

The numerical method used is based on the mathematical model which considers linearization of the term giving the vapour exchanged at the boundaries in terms of temperature and moisture content and the introduction of generic algorithm to simultaneously solve the governing equations for each time step. The model considered all other surfaces of the porous soil as adiabatic and impermeable apart from the upper surface but however did not take into account convection and radiation heat transfer in the pores nor the sensible heat transferred by the liquid and vapour phases.

2.1. Governing equations

The governing partial differential equations to model heat and mass transfer through porous media are based on the highly disseminated theory proposed by Philip and de Vries (1957). The expression for the energy conservation equation is

$$\rho_0 c_m(T, \theta) \frac{\partial T}{\partial t} = \frac{\partial}{\partial x} \left(\lambda(T, \theta) \frac{\partial T}{\partial x} \right) - L(T) \frac{\partial}{\partial x} (j_v) \quad (1)$$

while that of the mass conservation is given as

$$\frac{\partial \theta}{\partial t} = - \frac{\partial}{\partial x} \left(\frac{j}{\rho_l} \right) \quad (2)$$

where ρ_0 is the solid matrix density (Kg m^{-3}); c_m , the mean specific heat ($\text{J kg}^{-1} \text{K}^{-1}$); T , temperature ($^{\circ}\text{C}$); t , time (s); λ , thermal conductivity ($\text{W m}^{-1} \text{K}^{-1}$); L , latent heat of vaporization (J kg^{-1}); θ , volumetric moisture content ($\text{m}^3 \text{m}^{-3}$); j_v , vapour flow ($\text{kg m}^{-2} \text{K}^{-1}$); j , total flow ($\text{kg m}^{-2} \text{K}^{-1}$), which is the sum of the liquid flow, j_l ($\text{kg m}^{-2} \text{K}^{-1}$) and j_v ; ρ_l , the water density (kg m^{-3}). The vapour flow density is written as

$$\frac{j_v}{\rho_l} = -D_{Tv}(T, \theta) \frac{\partial T}{\partial x} - D_{\theta v}(T, \theta) \frac{\partial \theta}{\partial x} \quad (3)$$

while the equation expressing the total mass flow density is

$$\frac{j}{\rho_l} = -D_T(T, \theta) \frac{\partial T}{\partial x} - D_{\theta}(T, \theta) \frac{\partial \theta}{\partial x} \quad (4)$$

with $D_T = D_{Tl} + D_{Tv}$ and $D_{\theta} = D_{\theta l} + D_{\theta v}$, where D_{Tl} is the thermal liquid diffusivity, D_{Tv} , thermal vapour diffusivity, $D_{\theta l}$, isothermal liquid diffusivity, $D_{\theta v}$, isothermal vapour diffusivity, D_T , mass transport coefficient associated to a temperature gradient ($\text{m}^2 \text{s}^{-1} \text{ } ^{\circ}\text{C}^{-1}$) and D_{θ} , mass transport coefficient associated to a moisture content gradient ($\text{m}^2 \text{s}^{-1}$).

2.2. Boundary conditions

A one-dimensional physical soil domain whose depth, H , is along the vertical x -coordinate was considered. The lower surface of the domain is at $x = 0$, while the upper surface directly exposed to short and long-wave radiations, convection heat transfer, and phase change as boundary conditions is at $x = H$. All other surfaces were all considered adiabatic and impermeable.

Hence the energy balance at $x = H$ becomes

$$\left(\lambda(T, \theta) \frac{\partial T}{\partial x} \right)_{x=H} + (L(T) j_v)_{x=H} = h(T_{\infty} - T_{x=H}) + \alpha q_r + L(T) h_m (\rho_{v, \infty} - \rho_{v, x=H}) - \epsilon R_{lw} \quad (5)$$

While the mass balance at $x = H$ is expressed as

$$\left(D_{\theta}(T, \theta) \frac{\partial \theta}{\partial x} + D_T(T, \theta) \frac{\partial T}{\partial x} \right)_{x=H} = \frac{h_m}{\rho_l} (\rho_{v, \infty} - \rho_{v, x=H}) \quad (6)$$

where $h(T_\infty - T_{x=H})$ represents the heat exchanged by convection with the external air, described by the surface conductance (h), αq_r is the absorbed short-wave radiation and $L(T)h_m(\rho_{v,\infty} - \rho_{v,x=H})$, the phase change energy term. α is the solar absorptivity while the mass convection coefficient h_m is related to h by the Lewis relation. R_{lw} is the long-wave radiation while \mathcal{E} represents the surface emissivity. The vapour concentration difference between the porous surface and air, $\Delta\rho_v$ on the right hand sides of eqs. (5) and (6) is normally determined by using the values of previous iterations for temperature and moisture content, thereby generating additional instability. Mendes *et al.* (2002) calculated the vapour flow, independent of previous temperatures and moisture contents, by linearizing the term $\Delta\rho_v$ as a linear combination of temperature and moisture content, i.e.

$$(\rho_{v,\infty} - \rho_v(s)) = C_1(T_\infty - T(s)) + C_2(\theta_\infty - \theta(s)) + C_3 \tag{7}$$

with

$$C_1 = A \frac{M}{\mathfrak{R}} \phi, C_2 = \frac{M}{\mathfrak{R}} \left(\frac{P_s(s)}{T(s)} \right)^{pr} \left(\frac{\partial \phi}{\partial \theta(s)} \right)^{pr}, C_3 = \frac{M}{\mathfrak{R}} \left\{ \left(\frac{P_s(s)}{T(s)} \right)^{pr} R(\theta^{pr}(s)) + \phi_\infty (R(T_\infty) - R(T^{pr}(s))) \right\},$$

where R is a residual function of (P_s/T) ; P_s , saturated pressure (Pa); \mathfrak{R} , universal gas constant ($\text{Jkmol}^{-1}\text{K}^{-1}$); M , molecular mass (kgkmol^{-1}); ϕ , relative humidity; ``*pr*``, previous iteration, and A is the straight line coefficient from the approximation, $(P_s/T) = AT + B$.

2.3. Discretization

The control-volume formulation method (Patankar, 1980) was used to discretize the governing equations by using the control - difference scheme (CDS) as the spatial interpolation method and the time derivatives are integrated using a fully implicit approach. The MultiTriDiagonal-Matrix Algorithm (Mendes and Philippi, 2004) was used to solve a 1D model whereby, the dependent variables were obtained simultaneously, avoiding numerical divergence caused by the evaluation of coupled terms from previous iteration values.

2.4. Hygroscopic properties

The sorption isotherms were compared as shown in Fig. (1) where the sandy silt, sand and artificial backfill are material soils used by Oliveira *et al.* (1993) and loamy sand is from experimental site in Nigeria. Following the close range in values of sorption isotherms and thermal conductivity as shown in Fig. 2 for the experimented soil and sandy silt, the transport coefficients for tropical sandy silt obtained from Oliveira *et al.* (1993) were therefore used for the simulation processes.

Table 1 Dry-basis material properties

Bulk density (gcm^{-3})	Porosity (-)	% Sand	% Silt	% Clay
1.28	0.517	80	14	6

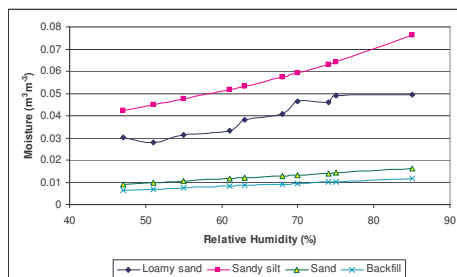


Figure 1. Soil sorption isotherms

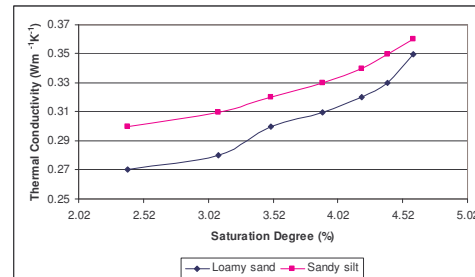


Figure 2. Thermal conductivity for sandy silt and loamy soil

3. Materials and Methods

3.1. Experimental measurement

The experimental site is located near the campus of the University of Abeokuta, which is in the moderately hot, humid tropical climatic region of the South-Western Nigeria, (7° 30'N, 3° 48'E). It belongs to the derived savanna zone and its annual rainfall is about 1200 mm. Based on the American Standard for Testing and Materials, the soil textural characteristics at the bare upper surface was loamy sand, and can be classified as Alfisol. The parent materials consisted of alluvial deposits in the valley and coarse grained granitic material in the upland. Humid tropical soils usually have moderate to high permeability under natural conditions but susceptible to slaking and development of impermeable crust upon action of raindrops. The large duration of the geologic age, extremes of climate and wide differences in parent materials are often the reasons for the great contrast of soil properties in the humid tropics from other soils elsewhere. The weather data consisting of solar radiation, relative humidity, outdoor temperature and evaporation covering the period of the experiment for the city of Abeokuta, 150 m above sea level, was obtained from the Nigerian Meteorological Centre. The rainy season usually lasts from March/April to October/ November and the dry season lasts for the remaining part of the year, October/November till March/April. The mean monthly temperature varies from 23 °C in August to 36 °C in March. The temperature is relatively high during the dry season with the mean about 30 °C. The harmattan, brought in by the north-easterly winds from December to February, has ameliorating effects on the dry season high temperatures. Low temperature is experienced during the rains, especially between July and August when the temperatures could be as low as 24°C. The relative humidity is usually high, ranging from 76 % in February to 88 % in July, with low precipitation in August. Measurements were made on the site (0.3 m × 0.3 m), with no vegetation cover, at periodic hours 06:00, 08:00, 10:00, 12:00, 14:00, 15:00, 16:00, 18:00, 20:00 and 22:00, from October 28 to November 1. Boul *et al*, (1990) noted that the common trend about all tropical soils is their lack of seasonal soil temperature variation, and that field experiments conducted in any period of the year may give sufficient information about the existing trend of soil temperature distributions. Temperature distributions were measured using a KD2 thermocouple sensor, which was inserted horizontally just at the soil surface for instantaneous measurements.

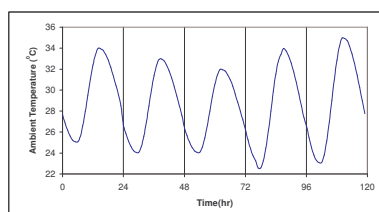


Figure 3. Outdoor temperature daily variation

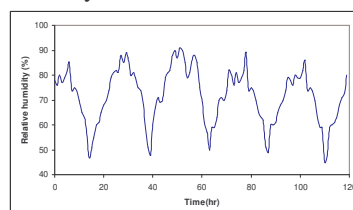
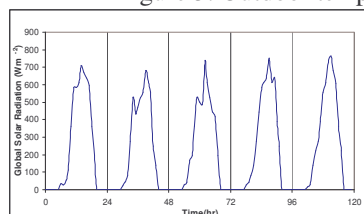


Figure 4. Daily variation of solar radiation Figure 5. Relative humidity daily variation

Moisture content evolution was determined by using the pre-determined average bulk density of triplicate core samples, carefully taken from the surface and oven dried at 105 °C for 24 h. The samples were taken in sealed columns to avoid evaporation, while all the weight measurements were made with a sensitive digital balance to enhance accuracy. Averaging of temperatures and sample weights, and weighing all samples to 0.001 g on a direct reading balance for each measurement helped to minimize the errors. The temperature measurements were also enhanced with a measurement accuracy of ± 0.05. Gravimetric water contents were converted to the volumetric basis by multiplying by the bulk density.

3.2. Numerical simulation

The weather data for the city of Abeokuta was used as the boundary condition at the upper surface of the soil with a constant convection heat transfer coefficient of 10 Wm⁻¹K⁻¹, and emissivity of 0.3. The other surfaces were considered adiabatic and impermeable. Other parameters like grid thickness, pre-simulation or warm-up period, time step, solar absorptivity and long wave radiation loss were varied to determine their influence on the accuracy of the numerical simulation as shown in Tabs. (2) and (3).

Numerical tests with varying parameters for temperature are shown in Tab. 2 where the surface node temperatures and the corresponding next-node temperatures, i.e., grid nodes 1 and 2 were computed under different conditions. On the other hand, because moisture content determined gravimetrically were actually the average moisture contents from core samples taken from the surface, simulated values of moisture contents for the first two or three sections, depending on the thickness, were therefore averaged and analyzed as shown in Tab. 3. Numbers in parentheses represent the nodes that were averaged for moisture content, and the actual nodes tested for temperatures. A temperature of 30 °C and a volumetric water content of

0.04412 m³m⁻³ corresponding to a relative humidity of 50 % were considered as initial condition for the soil. Since we are interested in a one-dimensional flow at the upper surface, a 5-m depth soil was simulated.

The results displayed at the end of the simulation represent the profiles of temperature and moisture content of the node at the centre of the domain surface, and were further analyzed over the 120-hour period of investigation. The varying parameters were selected because accurate determination of the temperature and moisture content profiles especially at the surface depends strongly on grid size refinement, time step and period of warm-up (Santos and Mendes, 2005).

Table 2 Numerical tests for temperature with varying parameters

Numerical Tests	Values in	Time Step (min)	Grid	R _{iw} (Wm ⁻²)	Warm-up Period (yrs)
	Grid Nodes		Thickness (cm)		
T1 (1) α = 0.5	Node 1	60	1.250	100	10
T1 (2) α = 0.5	Node 2	60	1.250	100	10
T2 (1) α = 0.5	Node 1	60	0.625	30	3
T2 (2) α = 0.5	Node 2	60	0.625	30	3
T3 (1) α = 0.5	Node 1	20	0.250	100	1
T3 (2) α = 0.5	Node 2	20	0.250	100	1
T4 (1) α = 0.5	Node 1	10	0.250	50	1
T4 (2) α = 0.5	Node 2	10	0.250	50	1
T5 (1) α = 0.5	Node 1	30	0.500	50	1
T5 (2) α = 0.5	Node 2	30	0.500	50	1
T6 (1) α = 0.8	Node 1	30	0.500	50	1
T6 (2) α = 0.8	Node 2	30	0.500	50	1

Table 3 Numerical tests for moisture content with varying parameters

Numerical Tests	Mean values in Grid Nodes	Time Step (min)	Grid Thickness (cm)	R_{lw} (Wm^{-2})	Warm-up Period (yrs)
$\theta 1$ (1.2) $\alpha = 0.5$	Nodes 1 - 2	60	1.250	100	10
$\theta 2$ (1.2) $\alpha = 0.5$	Nodes 1 - 2	60	0.625	30	3
$\theta 3$ (1.2) $\alpha = 0.5$	Nodes 1 - 2	20	0.250	100	1
$\theta 3$ (1.2.3) $\alpha = 0.5$	Nodes 1 - 3	20	0.250	100	1
$\theta 4$ (1.2) $\alpha = 0.5$	Nodes 1 - 2	10	0.250	50	1
$\theta 4$ (1.2.3) $\alpha = 0.5$	Nodes 1 - 3	10	0.250	50	1
$\theta 5$ (1.2) $\alpha = 0.5$	Nodes 1 - 2	30	0.500	50	1
$\theta 5$ (1.2.3) $\alpha = 0.5$	Nodes 1 - 3	30	0.500	50	1
$\theta 6$ (1.2) $\alpha = 0.8$	Nodes 1 - 2	30	0.500	50	1
$\theta 6$ (1.2.3) $\alpha = 0.8$	Nodes 1 - 3	30	0.500	50	1

4. Results and Discussion

4.1. Error analysis and model validation

Experimental errors inherent in the gravimetric measurement of soil water content arose from sampling of cores to determine the bulk densities, while instantaneous measurements of temperature also gave rise to some errors. The validation or otherwise of the model was tested by calculating and comparing the errors over the entire period of investigation, for each numerical test. The percentage relative errors calculated were compared with time as shown in Figures 6 – 10 for temperatures and 11 – 14 for moisture contents. Average percentage errors for numerical temperature tests T1 (1), T1 (2), T2 (1), T2 (2), T3 (1), T3 (2), T4 (1), T4 (2), T5 (1), T5 (2), T6 (1) and T6 (2) were 10.26, 5.34, 9.24, 7.10, 8.16, 8.11, 6.86, 6.28, 8.32, 6.40, 8.32 and 6.40 respectively while for moisture tests, the average percentage errors were 12.08, 10.19, 10.06, 13.13, 9.04, 12.53, 9.92, 14.06, 9.92 and 14.06 for $\theta 1$ (1.2), $\theta 2$ (1.2), $\theta 3$ (1.2), $\theta 3$ (1.2.3), $\theta 4$ (1.2), $\theta 4$ (1.2.3), $\theta 5$ (1.2), $\theta 5$ (1.2.3), $\theta 6$ (1.2) and $\theta 6$ (1.2.3) respectively.

The second node had lower errors for temperature than the first, though as the time step and the grid size reduced, the values for first and the second nodes were getting closer as shown in Figs. (8) and (9). Averaging the first two nodes also increased the accuracy for moisture content more than the first three nodes. With an increase in solar absorptivity from 0.5 to 0.8, there was no noticeable change as same error average values were recorded for T5 (1) and T6 (1), and T5 (2) and T6 (2). Similarly same values of error averages were returned for θ_5 (1.2) and θ_6 (1.2), and also for θ_5 (1.2.3) and θ_6 (1.2.3). The sensitivity of the model to grid size refinement and time step was pronounced as smaller grid sizes and time steps yielded lowest errors for both temperature and moisture contents. Pre-simulation period also influenced the temperature model where lower error was observed with 10 years period as shown in Fig. (6).

The effect of long wave radiation loss was also noticed when for instance, in T3 (2) and T4 (2) as shown in Figs. (8) and (9), where both R_{lw} and the time step were reduced by 50 % and other parameters were kept constant, yielding an error reduction of 23 %. The percentage relative errors were also computed for each day to study effects of atmospheric variables on the model performance. Errors were much higher on day 3 as compared to other days for the numerical simulation of temperature evolution. This may be attributed to the fact that the location point for the outdoor temperature and global radiation measurement for the city was not near to the experimental site which may be subject to a micro climate on day 3. On the other hand, day 3 had the lowest errors in numerical simulation of moisture content, while day 2 and day 4 had relatively high errors. With respect to the time of the day, there were more errors recorded during the night for the moisture simulation and temperature simulation. At the peaks of temperatures however, temperature sub-model agreed more fairly well than the moisture sub-model with the exception of day 3.

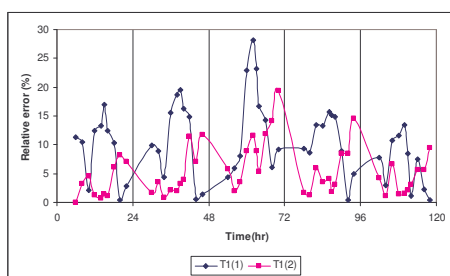


Figure 6. Relative errors for T1 (1) and T1 (2)

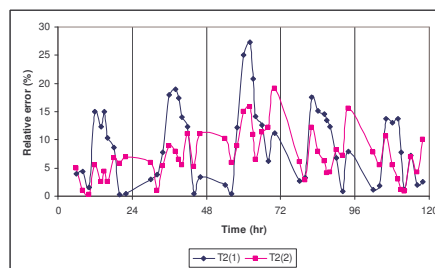


Figure 7. Relative errors for T2 (1) and T2 (2)

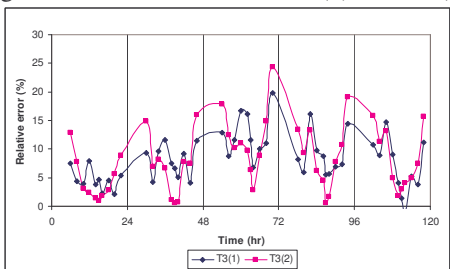


Figure 8. Relative errors for T3 (1) and T3 (2)

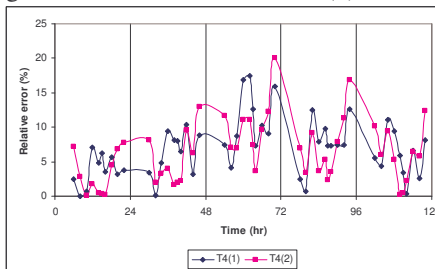


Figure 9. Relative errors for T4 (1) and T4 (2)

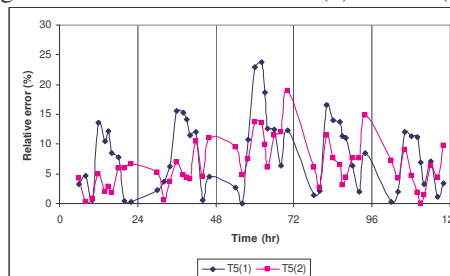


Figure 10. Relative errors for T5 (1) and T5 (2)

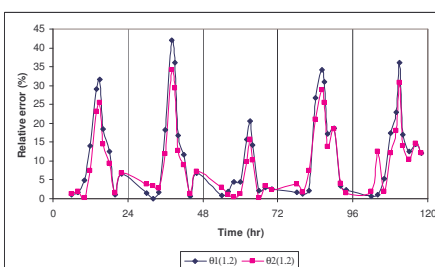


Figure 11. Relative errors for θ_1 (1.2) and θ_2 (1.2)

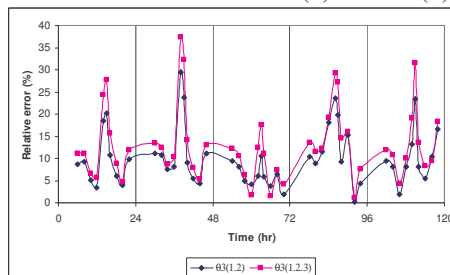


Figure 12. Relative errors for θ_3 (1.2) and θ_3 (1.2.3)

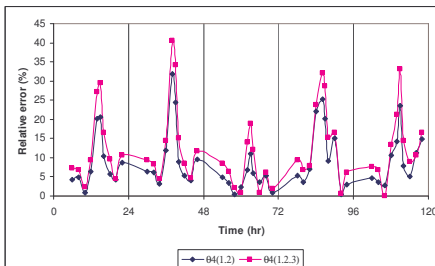


Figure 13. Relative errors for θ_4 (1.2) and θ_4 (1.2.3)

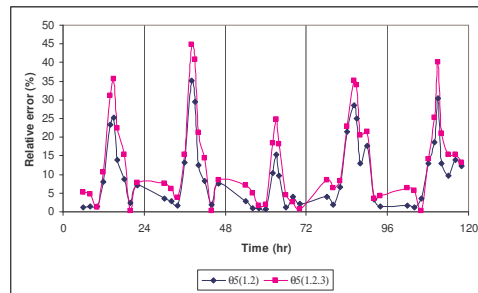


Figure 14. Relative errors for 05 (1.2) and 05 (1.2.3)

The discrepancy can be attributed to some irregularities in the global radiation pattern especially on day 3 because sands are highly porous and permeable, making them strongly responsive to changes in atmospheric variables. A likely reason also for the inconsistency is the assumed transport coefficients which were not directly measured. The test case with lowest errors of 5.34 and 9.04 for both temperatures and moisture contents respectively was selected for detailed descriptions. For the selected numerical case as further described in Figs. (15) and (16), the average absolute error was 1.894 for soil temperature and 0.003172 for soil moisture content, while the average relative errors for soil temperature and moisture contents were 0.053426 and 0.090426 respectively. Daily average errors were 3.37, 4.76, 9.16, 5.31 and 4.11 % for temperatures and 6.61, 11.14, 4.48, 11.12, and 9.86 % for moisture contents from day 1 to day 5 respectively. Day 3 had the highest error for temperature and the lowest for moisture content.

4.2. Soil temperature

The soil temperature sub-model was tested by comparing the observed data with simulated model results. The correlation coefficient was determined as 0.9479, indicating that both the predicted values and observed data followed same diurnal fluctuation trend. The maximum percentage relative error of 19.39 % was recorded at 10 p.m. on day 3, while the minimum of 0.07 % was recorded at 6 a.m. on day 1. The model overestimated the temperatures early in the morning except only for day 1, and especially late at night. Consequently, greater errors of the model were recorded at night hours while the model recorded lower errors in the morning suggesting that measurement errors could have occurred since there was no radiation at such period. At the peak hours also, the model overestimated temperatures with the exception of day 5.

Figure (3) presents the outdoor temperatures from 28th October to 1st November indicating that the ambient temperatures varied from a minimum of 22.60 °C to a maximum of 34.90 °C, with amplitude of 6.15 °C. Figure (4) gives the solar radiation at the experimental site, where the daily peak usually falls between 1 p.m. and 2 p.m. The monthly mean global solar radiation is usually high in the months of October and November which most often signifies the inception of the dry season in this West African sub region (Iziomon and Aro, 1999).

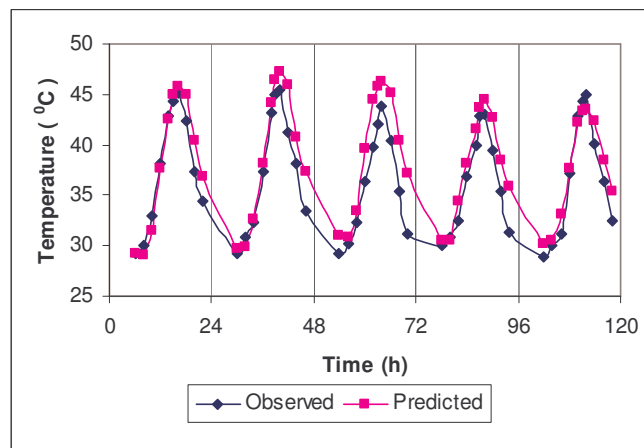


Figure 15. Observed versus predicted soil temperature evolution

Comparing the simulated results with ambient measurements of air temperature and solar radiation, the average values of temperature at the surface were strongly associated with daily average values of the prevailing atmospheric variables. The correlation between the hourly simulated and observed spatial and temporal distributions of temperature at the surface are compared as shown in Fig. (15). The amplitude of fluctuation was thus 9.055 °C for the predicted values and 8.25 °C for the measured values. This is as expected because, at the surface, the period of soil temperature variation is minimal and the amplitude of temperature fluctuation is remarkably high.

The observed surface temperature pattern can be attributed to the hygrothermal behaviour of sandy soil which is characterized by high night-time condensation and rapid day-time warm up because of low thermal capacity. There was also a high latent heat flux because moisture is easily released into the air. Since temperature variational trend is a common phenomenon in all tropical soils, it becomes necessary to compare with other tropical climates.

Previous researches have recorded same trend for other tropical regions of Southern Brazil and South-Eastern India (Derpsch et al., 1985; Dalmago et al., 2004; Ghuman and Lal, 1981; Anandakumar et al., 2001). Similar experiments to simulate temperature and moisture content in some soils in the Po Valley of Northern Italy and South Ticino area of Switzerland using the land surface process model also observed same variational fluctuations (Cassardo et al., 1995, 2002).

4.3. Soil water content

The amount of soil water which is held by attraction of water molecules to each other and to soil particles by capillarity changes over time affects its availability. Figure (5) shows the prevailing relative humidity from October 28 to November 1. The outdoor relative humidity varied from a minimum of 45 % to a maximum of 91 % within the period of experimental investigation. The simulated values were plotted with observed data at the periodic hours of measurement as shown in Fig. (16). Soil water content decreased at the surface during the daytime because of evaporation and slightly increased during the night.

As temperature increased, the hydraulic conductivity which is strongly related to both water content and soil temperature also increased while the soil water capacity decreased. The data also indicate the wide range of water contents encountered at the surface during a diurnal course of experimental investigation. On day 2 for instance, observed water content decreased by 47 % between 06:00 and 15:00 hours, recovered during the night, and again dried rapidly the next day. Similarly on day 4, a decrease of 46 % was observed while the same pattern was exhibited through out the duration of both the numerical computation and experimental observation.

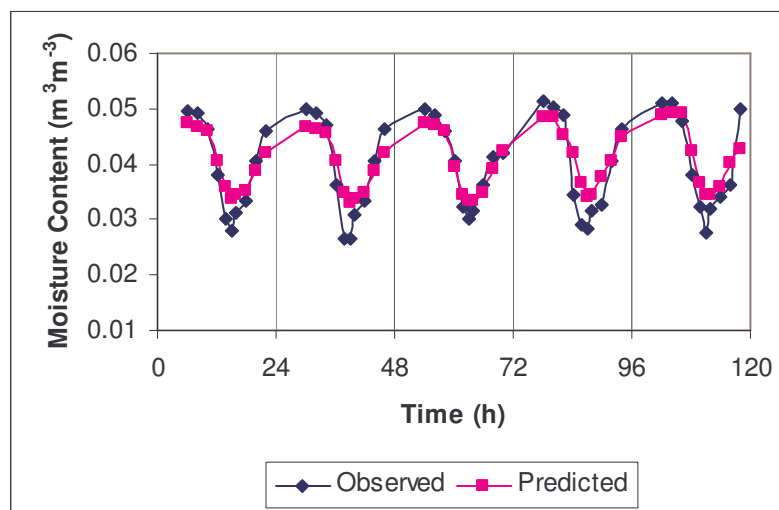


Figure 16. Observed versus predicted soil moisture content evolution

The measured volumetric moisture contents were low, partly due to the fact that the dry season had already commenced, and also because of the increased sand fractional percentage which decreased soil moisture. Soil water holding capacity has long been discovered to vary remarkably with soil texture. The finer the soil particles, the larger the soil water capacity which is usually less than 10 % for sandy soil (Carson, 1969; Scheroeder, 1984). The difference can also be attributed to the assumed moisture transport coefficients which were not directly measured for the simulated soil. To test the moisture content sub-model, the observed results were compared with the predicted values and the correlation coefficient was calculated as 0.9397 indicating that both were in phase. The maximum percentage relative error of 31.80 % was recorded at 2 p.m. on day 2, while the least was 0.41 % at 10 a.m. on day 3.

The differences between the predicted and observed volumetric water content were all positive at the extremes of temperature on all the days of the experimental investigation, indicating that the model overestimated the moisture content during the day time. Unlike the temperature sub-model, the moisture sub-model underestimated volumetric water contents early in the morning and also especially late at night, with the exception of day 3, but also overestimated moisture at the sunshine peak hours for all the days of investigation.

However, while on day 3, temperature was overestimated at the peak hours of sunshine, the predicted moisture contents agreed better with measured values whereas on days 1 and 5, predicted and measured temperature agreed fairly well but moisture was much overestimated. Mollerstrom (2004) also noticed some discrepancies in the investigation of DAYCENT land surface model to compare the simulated soil moisture and temperature with observed data in semiarid Sudan and explained that the performance of the model can be attributed to some irregularities in the weather pattern.

5. Conclusion

Evolution of temperature and soil water at the surface displayed existing patterns comparable with other researchers in the tropical climates and elsewhere. There was a fairly good agreement between the measured and predicted values of surface temperature and moisture content distributions, with both following same diurnal fluctuation trend and consequently correlation coefficients greater than 0.9. While the model underestimated the soil moisture content at 6 a.m. and 10 p.m., the measured temperatures were however overestimated. When compared to moisture content, average errors for temperature were low resulting in a minimal absolute difference in amplitude of 0.81°C. High porosity and permeability characteristics of sandy soils generally affect their response to changes in atmospheric variables, especially global radiation and relative humidity, thereby introducing some inconsistency into the performance of the model. The sensitivity of the numerical model was very high to the choice of simulation parameters especially time step and grid size refinement.

6. Acknowledgements

The authors thank the Brazilian Research Council (CNPq) of the Secretary for Science and Technology of Brazil for supporting this work. We also gratefully acknowledge Mr. Olajide Adefuye of Nigerian Meteorological Centre for assisting us with weather data, Eng. Marluz Jonsson of the Pontifical Catholic University of Parana, Brazil for his unquantifiable moral supports and Eng. Roberto Zanetti Freire who assisted with programming. This paper was written during the first author's postdoctoral fellowship period in Brazil.

***Corresponding author. Permanent address: Physics Department, University of Agriculture, Abeokuta, Nigeria; Tel.: +234 803 883 0290; E-mail address: olukayodewumi@yahoo.com**

7. References

- Anandakumar, K., Venkatesan, R. and Prabha, T. V., 2001, "Soil thermal properties at Kalpakkam in coastal south India", Proc. Indian Acad. Sci., (Earth Planet. Sci.), Vol. 110, No. 3, pp. 239-245.
- Buol, S. W., Sanchez, P. A., Weed, S. B. and Kimble, J. M., 1990, "Predicted impact of climatic warming on soil properties and use", In: Impact of carbon dioxide, trace gases, and climate change on global agriculture. ASA Special Publication, Vol. 53, pp. 71-82.
- Carson, M. A., 1969, "Soil moisture", Chorley, R.J., (ed.) Introduction to physical geography, Methuen 7 Co., London Vol. 101.
- Cassardo, C., Ji, J. J. and Longhetto, A. 1995, "A study of the performance of a land surface process model (LSPM)", Boundary Layer Met., Vol. 72, pp. 87-121.
- Cassardo, C., Balsamo, G. P., Cacciamani, C., Cesari, D., Peccagnella, T. and Pelosini, R., 2002, "Impact of soil surface moisture initialization on rainfall in a limited area model: a case study of the 1995 South Ticini flash flood", Hydrol. Process., Vol.16, pp. 1301-1317.
- Cassel, D. K., Nielson, D. R. and Biggar, J. W., 1969, "Soil-water movement in response to imposed temperature gradients", Soil Sci. Soc. Amer. Proc., Vol. 33, pp. 493-500.
- Dalmago, G. A., Bergamaschi, H., Comiran, F., Bianchi, C. A. M., Bergonci, J.I. and Hechler, B. M. M., 2004, "Soil temperature as a function of soil tillage systems", ISCO 2004, 13th Int. Conservation Org. Conf. – Brisbane.
- Derpsch, R., Sidiras, N. and Heinzmann, F. Z., 1985, "Manejo do solo em coberturas verdes de inverno", Pesquisa Agropecuária Brasileira. Vol. 20, pp. 761-773.
- Deru, M. P. and Kirkpatrick, A. T., 2002, "Ground-coupled heat and moisture transfer from building, Part 1: Analysis and modeling", J. Solar Energy Engr., Vol. 124, pp. 10-16.
- de Vries, D. A., 1958, "Simultaneous transfer of heat and moisture in porous media", Trans. Amer. Geophys. Union, Vol. 39, pp. 909-916.
- de Vries, D. A., 1987, "The theory of heat and moisture transfer in porous media revisited", Int. J. Heat Mass Transfer, Vol. 30, No.7, pp. 1343-1350.
- Ghuman, B. S. and Lal, R., 1981, "Predicting diurnal temperature regime of a tropical soil", Soil Sc., Vol. 132, pp. 247-252.
- Griffol, J., Gasto, J. M. and Cohen, Y., 2005, "Non-isothermal soil water transport and evaporation", Adv. Water Res., Vol. 28, pp. 1254-1266.
- Iziomon, M. G. and Aro, T. O., 1999, "On the annual and monthly mean diurnal variations of diffuse solar radiation at a meteorological station in West Africa", Meteor. Atmosp. Phys., Vol. 69, pp. 223-230.
- Jackson R, D., Reginato, R. J., Kimball, B. A. and Nakayama, F. S., 1974, "Diurnal soil-water evaporation: Comparison of measured and calculated soil-water fluxes", Soil Sci. Soc. Amer. Proc., Vol. 38, pp. 863-866.
- Jury, W. A. and Letey, J., 1979, "Water vapour movement in soil: Reconciliation of theory and experiment", Soil Sci. Soc. Amer. Proc., Vol. 43, pp. 823-827.
- Kerestecioglu, A. and Gu, L., 1989, "Incorporation of the effective penetration depth theory into TRNSYS", Draft Report, Florida Solar Energy Center, Cape Canaveral, FL.

- Lu, J., Huang, Z. Z. and Han, X. F., 2005, "Water and heat transport in hilly red soil of southern China: Experiment and analysis", *J. Zhejiang Univ. SCI.*, Vol. 6B, No. 5, pp. 331-337.
- Lu, J., Huang, Z. Z. and Han, X. F., 2005, "Water and heat transport in hilly red soil of southern China: Modelling and Simulation", *J. Zhejiang Univ. SCI.*, Vol. 6B, No. 5, pp. 338-345.
- Mendes, N., Philippi, P. C. and Lamberts, R., 2002, "A new mathematical method to solve highly coupled equations of heat and mass transfer in porous media", *Int. J. Heat Mass Transfer*, Vol. 45, pp. 509-518.
- Mendes, N. and Philippi, P. C., 2003, "MultiTridiagonal matrix algorithm for coupled heat transfer in porous media: Stability analysis and computational performance", *J. Porous Media*, Vol. 7, No. 3, pp. 1-19.
- Mollerstrom, L., 2004, "Modelling soil temperature and soil water availability in semi-arid Sudan: Validation and testing", *Doctoral Dissertation*, Lund University, Sweden.
- Nassar, I. N. and Horton, R. 1989, "Moisture transport in unsaturated nonisothermal salty soil: Experimental results", *Soil Sci. Soc. Amer. J.*, Vol. 53, pp. 1323-1329.
- Nassar, I. N., Horton, R. and Globus, A. M., 1992a, "Simultaneous transfer of heat, moisture, and solute in porous media: II. Experiment and analysis", *Soil Sci. Soc. Am. J.*, Vol. 56, pp. 1357-1365.
- Nassar, I. N., Globus, A. M. and Horton, R., 1992b, "Simultaneous soil heat and water transfer", *Soil Sci.*, Vol. 154, No. 6, pp. 465-472.
- Oliveira, A. A. M., Freitas, D. S. and Prata, A. T., 1993, "Influencia das propriedades do meio nas difusividades do modelo de Philip e de Vries em Solos Insaturados", *Relatório de Pesquisa*, UFSC.
- Patankar, S. V., 1980, "Numerical heat transfer and fluid flow", New York: McGraw-Hill.
- Philip, J. R. and de Vries, D. A., 1957, "Moisture movement in porous materials under temperature gradients", *Trans. Amer. Geophys. Union*, Vol. 38, pp. 222-232.
- Przesmycki, Z. and Strumillo, C. 1985, "The mathematical modelling of drying process based on moisture transfer mechanism", *Drying '85*, pp. 126-134.
- Rubin, J., 1968, "Theoretical analysis of two-dimensional transient flow of water in unsaturated and partly saturated soils", *Soil Sci. Soc. Amer. Proc.*, Vol. 32, pp. 607-615.
- Santos, G. H. and Mendes, N., 2005, "Unsteady combined heat and moisture transfer in unsaturated porous soils", *J. Porous Media*, Vol. 8, No. 5, pp. 1-18.
- Scheroder, D., 1984, "Soils: facts and concepts", International Potash Institute, Bern, Switzerland, Translated from German and adapted by P.A. Gethin, 139p.
- Whitaker, S., 1977, "Simultaneous heat, mass and momentum transfer in porous media: a theory of drying", *Adv. Heat Transfer*, Vol. 13, pp. 119-203.
- Wu, J. and Nofziger, D. L., 1999, "Incorporating temperature effects on pesticide degradation into management model", *J. Environ. Qual.*, Vol. 28, pp. 92-100.
- Yamanaka, T., Takeda, A. and Shimada, J., 1998, "Evaporation beneath the soil surface: Some observational evidence and numerical experiments", *Hydrol. Processes*, Vol. 12, pp. 2193-2203.
- Yoon, H., Valocchi, A. J. and Werth, C. J., 2003, "Modelling the influence of water content on soil vapour extraction", *Vadoze Zone J.*, Vol. 2, pp. 368-381.

8. Copyright Notice

The authors are the only responsible for the printed material included in their paper.